Conf-951033--11

LA-UR-. 95-2535

Title: IMPROVING THE DIVERSITY OF MANUFACTURING ELECTRO-LUMINESCENT FLAT PANEL DISPLAYS

Author(s):

T.S. Moss	MST-7
J.A. Samuels	MST-7
D.C. Smith	MST-7
R.C. Dye	MST-7
C.F. Schaus	Planar Systems, Inc.
M. Delarosa	Planar Systems, Inc.

Submitted to: The 27th International SAMPE Technical Conference
October 9 - 12, 1995
Albuquerque, NM

DISTRIBUTION OF THIS DOCUMENT IS UNLIMITED

MASTER

RECEIVED
AUG 29 1995
OSTI

Los Alamos
NATIONAL LABORATORY

IMPROVING THE DIVERSITY OF MANUFACTURING ELECTROLUMINESCENT FLAT PANEL DISPLAYS

T. S. Moss, J. A. Samuels, D. C. Smith, and R. C. Dye
Los Alamos National Laboratory, Los Alamos, NM 87545
and
C. F. Schaus and M. Delarosa
Planar Systems, Inc. Beaverton, OR 97006

ABSTRACT

Crystalline calcium thiogallate with a cerium dopant has been deposited by metal-organic chemical vapor deposition (MOCVD) at temperatures below 600° C on a low cost glass substrate. An EL luminance of 1.05 fL was observed 40 volts above threshold at 60 Hz. This is more than an order of magnitude improvement over earlier crystalline-as-deposited thiogallate materials. These results pave the way for the use of MOCVD as a potential method for processing full color thin-film electroluminescent (TFEL) flat panel displays. The formation of the $CaGa_2S_4$:Ce phosphor requires precise control over a number of deposition parameters including flow rates, substrate temperature, and reactor pressure. The influence of these parameters will be discussed in terms of structure, uniformity, and TFEL device performance.

KEY WORDS: Electroluminescent, Phosphor, and MOCVD

1. INTRODUCTION

The development of commercially viable flat panel displays has become a priority for many U.S. agencies and companies. One effort for the development of flat panel displays has been in the cultivation of an efficient and reliable blue emitter. One such material is cerium-doped calcium thiogallate ($CaGa_2S_4$:Ce).

The lack of a satisfactory blue phosphor having sufficiently high luminances at low power has hampered the development of high resolution flat panel displays. Recently, a new series of blue emitting materials have been investigated for use in thin film electroluminescent (TFEL) devices.(1-3) These phosphors are based on a series of alkaline earth thiogallate host materials of the form MGa_2S_4:RE where M can be either calcium, strontium, zinc, or barium and RE is a rare earth ion. A full-color VGA TFEL panel using $CaGa_2S_4$:Ce as the blue phosphor has recently been fabricated and tested.(1) This FPD provided a luminance of 2.92 fL at 60 Hz. The enhanced blue in this display allowed its color capabilities to approach those of the conventional CRT.

The method of depositing the phosphor onto the display panels in these test devices has been sputtering. Unfortunately the phosphor as deposited does not possess the crystalline properties required for optimum luminance. The crystalline structure is achieved by subsequent annealing of the as-deposited material. Although this post deposition anneal provides the desired crystal structure, it occurs above the melting temperature of ordinary glass. Consequently, the implementation of these phosphors requires the use of glasses capable of withstanding high temperatures, adding to the cost of the final display unit.

To circumvent this problem, other deposition techniques are being considered for the phosphor. One method under consideration is metal-organic chemical vapor deposition (MOCVD). This technique offers several advantages. First, it is a method in which complex thin film structures can be routinely deposited. Not only can the stoichiometry of the coating be controlled, but crystalline films can be obtained at deposition temperatures below 600°C. Second, the simple apparatus and reasonably high deposition rates also makes MOCVD attractive as a manufacturing processes. Consequently, this technique is promising as an alternative technique to obtain crystalline phosphors.

Calcium thiogallate is a material which can be synthesized through the direct reaction of calcium sulfide (CaS) and gallium sulfide (Ga_2S_3), according to the overall reaction: (5)

$$CaS + Ga_2S_3 \rightarrow CaGa_2S_4$$

The crystalline phase of $CaGa_2S_4$ is orthorhombic (space group: Fddd) with 32 formula units per unit cell. The determined unit cell dimensions are listed as a=20.086, b=20.086, and c= 12.112 Å. It has a melting temperature of 1410 K; a density of 3.37 g/cm^3; a microhardness of 31.8×10^6 Pa; and a resistivity of 2×10^{10} ohm·cm.(5)

Calcium thiogallate has been previously investigated as a possible phosphor for conventional CRT screens.(4) This compound was formulated by grinding together stoichiometric amounts of the appropriate alkaline earth carbonates and rare earth oxides and heating the mixture in a hydrogen sulfide environment at around 1000°C. More recently, calcium thiogallate was synthesized by heating a stoichiometric mixture of Ga_2S_3 and CaS to 1400°C.(5)

The production of $CaGa_2S_4$:Ce for use in flat panel displays requires a production technique which can reliably apply the material in thin layers with high performance tolerances. This method must also be relatively inexpensive and able to be interfaced with current production-type techniques. The process of MOCVD appears to be especially well-suited to these criteria. MOCVD allows for low temperature deposition of thin films onto substrates, which is important for applying the phosphor to the glass substrates for use in screens and monitors. Further, when properly practiced, MOCVD allows for precise control over many aspects of the deposition, such as thickness, composition, and morphology. However, to this point there has been little work in the synthesis of $CaGa_2S_4$:Ce through the route of chemical vapor deposition.

2. EXPERIMENTAL

The $CaGa_2S_4$:Ce coatings produced at Los Alamos National Laboratory were deposited using an 8″ stainless steel horizontal reactor. The reactor was a warm wall, impinging jet design, heated using a 1 kW quartz lamp that was directed at the substrate through a quartz window at the end of the reactor. All reagent transport lines were constructed of stainless steel and heated to at least 10°C over the highest bubbler temperature. Substrates were obtained from Planar Systems, Inc., and were composed of 1″x2″piece of glass that was overcoated by indium tin oxide (ITO), aluminum titanium oxide (ATO), and zinc sulfide (ZnS) to allow for the electroluminescent properties to be measured following the deposition. A rectangular-cut silicon wafer, necessary for even heating of the substrate, was sandwiched between the substrate and a backing glass slide. The three layer substrate assembly was held within the gas flow by a clip-type arrangement. The temperature was measured at the top and the bottom of the substrate using two type K thermocouples, and the temperature differential was kept below 1.5°C by slight adjustments to the focus of the quartz lamp. The pressure within the reactor was monitored and controlled by an MKS transducer interfaced with a throttle valve.

The metal-organic reagents used for the deposition were metal beta-diketonates ($Ca(tmhd)_2$, $Ga(tmhd)_3$, $Ce(tmhd)_4$, where the tmhd group was 2,2,6,6-tetramethyl-3,5-heptanedionate). The reagents were purchased from Strem Chemicals and were freshly sublimed prior to loading into a stainless-steel bubbler. The transport rate of each reagent was controlled by independent heating of the bubbler and a carrier gas flow through the bubbler. The flow rate of the reagent was then the result of the vapor pressure of the solid reagent, the flow rate of the carrier gas, and the total pressure within the bubbler. Reagents were combined in a mixing manifold before entering the reactor. Hydrogen sulfide (H_2S) was introduced just prior to the entrance into the reactor.

Deposited films were initially characterized by x-ray fluorescence (XRF) and x-ray diffraction (XRD). The presence of $CaGa_2S_4$ was determined based on XRD patterns taken from a Rigaku rotating anode diffractometer at an incident angle of 20° with an INEL position sensitive detector. Peak positions were determined using the INEL software program on the raw pattern. The $CaGa_2S_4$ was confirmed by comparing the pattern against JCPDS Card 25-134. The XRF measurement was used to quantify the amounts of Ca, Ga, and Ce deposited. For all of the runs in this study except two, the deposition was found by XRF to be rich in gallium. The gallium was likely in the form of excess Ga_2S_3 since $CaGa_2S_4$ acts as a line compound.(5) Therefore, the ratio of Ce to Ca may be thought of as the degree of Ce doping into the $CaGa_2S_4$. Samples were returned to Planar Systems, Inc., for electroluminescent measurements (EL). The EL measurements of test pixels included the determination of the chromaticity of the luminescence, given in the form of C.I.E. numbers, and the brightness at 40 V over the turn on voltage and at 60 Hz.

The run conditions for samples presented within this study are summarized in Table 1. All experiments were done at 5 torr, for 20 minutes, and approximately 582°C in the reactor.

Table 1. Deposition conditions for the experiments presented in this paper are summarized. The bubbler conditions are given as temperatures, and the flow rates are for the Ar carrier gas.

Run	Temp	time	$Ca(tmhd)_2$		$Ce(tmhd)_4$		$Ga(tmhd)_3$	
	(C)	(min)	T(C)	Flow(sccm)	T(C)	Flow(sccm)	T(C)	Flow(sccm)
1	584.4	20	229	5.2	182	1.2	134	20
2	582.1	20	229	5.2	182	0	134	19.6
3	582.7	20	229	5.6	180	1.28	134	19.6
4	582.2	20	229	5.6	178	1.2	134	20
5	583.6	20	229	5.6	176	1.28	134	20
6	582.2	20	229	5.6	174	1.2	134	19.6
7	582.7	20	229	5.6	186	1.36	134	20
8	583.5	20	229	5.2	186	2.08	134	20
9	582.1	20	229	5.2	180	2.16	134	19.6
10	584.5	20	229	5.2	174	2.08	134	20
11	582.8	20	229	5.2	170	2.16	134	19.8
12	581.6	20	229	5.2	170	1.68	134	20
13	582.3	20	229	5.2	170	1.68	134	22.4
14	581.2	20	229	5.2	170	1.68	134	23.6
15	582	20	229	5.2	170	1.12	134	23.6
16	582.7	20	229	5.2	170	1.12	134	23.6
17	581.9	20	227	5.2	170	0.72	134	23.6
18	582.5	20	227	5.2	168	0.72	134	23.6
19	577	20	225	5.2	170	0.72	134	23.6
20	581.2	20	225	5.2	170	0.72	134	23.6

3. RESULTS AND DISCUSSION

The results for the experimental conditions listed in Table 1 are summarized in Table 2. In Table 2, unit cell volumes were estimated from the XRD patterns; XRF ratios were calculated using a calibration for elemental adsorption; C.I.E. numbers were converted into deltas using Equation 2; and brightness values were taken from the same spot as the C.I.E. measurements.

Table 2. Characterization of the samples described in Table 1 are shown

Run	XRD	XRF			C.I.E.			Bright. (fL)
	$V_{Est}(A^3)$	Ga/Ca	Ce/Ca	Ce/Ga	x	y	Delta	
1	4984.2	1.023	0.0465	0.0455	0.417	0.454	0.369	2.2
2	----	1.897	0.002	0.0011	-----	----	----	----
3	4961.7	1.296	0.0626	0.0483	0.4	0.31	0.273	0.78
4	----	0.634	0.0163	0.0258	-----	----	----	----
5	4898.1	1.715	0.0677	0.0395	0.168	0.232	0.037	0.35
6	4869.8	1.694	0.0593	0.035	0.217	0.293	0.115	0.27
7	5075.6	1.739	0.1551	0.0892	-----	----	----	----
8	4962.7	1.938	0.2406	0.1241	-----	----	----	----
9	4942.4	2.02	0.2087	0.1033	0.194	0.259	0.074	0.062
10	4927.3	2.057	0.1486	0.0722	-----	----	----	----
11	5014.9	1.784	0.0831	0.0466	0.158	0.233	0.034	0.34
12	4940.4	1.827	0.0596	0.0327	0.177	0.248	0.055	0.45
13	4900.3	2.145	0.0725	0.0338	0.161	0.229	0.031	0.26
14	4977.6	2.179	0.086	0.0395	0.323	0.391	0.258	0.15
15	4977.8	2.636	0.0518	0.0197	0.156	0.244	0.044	1.05
16	4944.3	2.624	0.0107	0.0041	0.257	0.508	0.326	1.2
17	4926.4	2.527	0.0126	0.005	-----	----	----	----
18	4842.1	5.166	0.0072	0.0014	0.162	0.238	0.04	0.08
19	4938.7	4.185	0.0234	0.0056	0.165	0.247	0.049	0.45
20	4980.2	5.551	0.0316	0.0057	0.328	0.312	0.21	0.35

The consistency of the processing for these samples is the first step in the determination of the quality of the process of MOCVD. Since the use of these types of reagents has not been widespread, information regarding their vapor pressure as a function of temperature is not readily available. Thus, the conditions of temperature and flow of carrier gas through the bubbler must be determined empirically. For this step, the raw results from the XRF measurements were used. The results of the amount of Ca deposited as a function of the temperature in the $Ca(tmhd)_2$ bubbler for a constant carrier flow of Ar through the bubbler are shown in Figure 1.

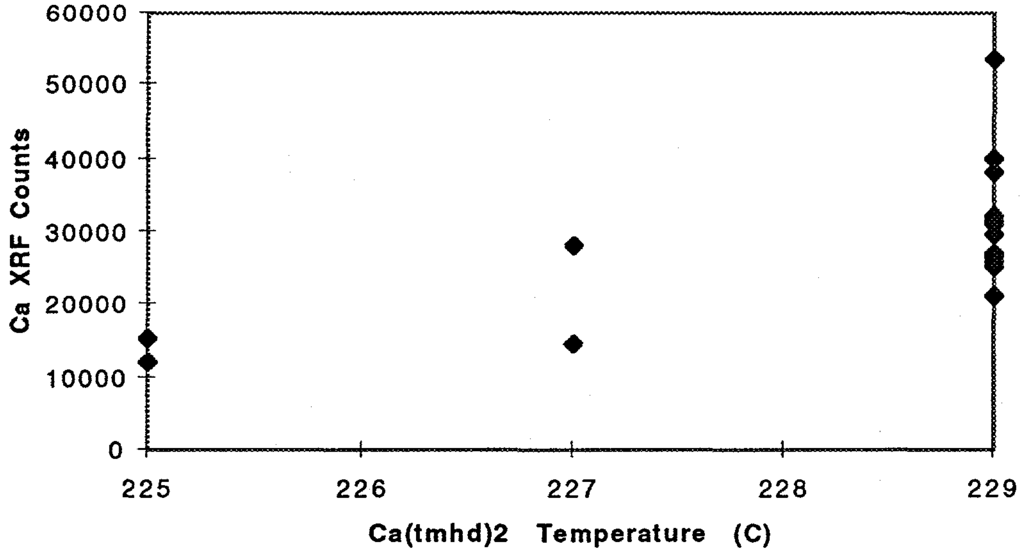

Figure 1. The number of Ca counts as determined by XRF increases as the temperature of the Ca(tmhd)$_2$ bubbler is increased.

The number of Ca counts can be seen to increase rapidly as the temperature increases. The shape of the curve shows an exponential type rise in the counts. This trend is expected due to the exponential relationship between vapor pressure and temperature, but some of this shape could possibly be attributed to a kinetic reaction effect. The same type of analysis may also be tried for the Ce(tmhd)$_4$. This plot is shown in Figure 2.

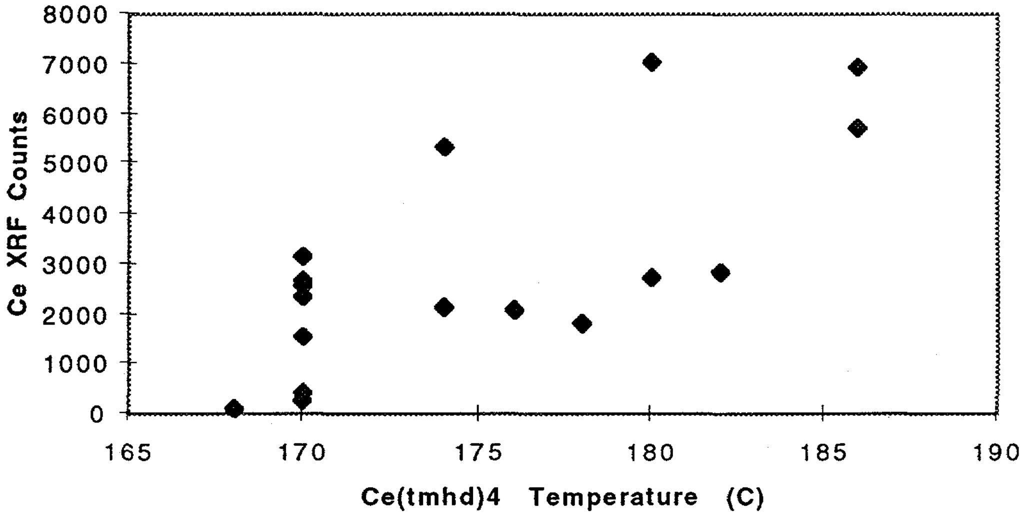

Figure 2. Increases in the Ce(tmhd)$_4$ temperature also increase the number of measured Ce XRF counts.

However, the graph of Ce counts does not show as well defined of a trend as did the Ca XRF counts in Figure 1. Part of this may be attributable to the low doping concentrations of Ce in the films (3-5%). This resulted in small Ce peaks which added a significant amount of uncertainty to the data shown in Figure 2.

For the analysis of the Ga counts, only two Ga(tmhd)$_3$ carrier flow rates were tried with the temperature in the bubbler held constant. Because of this, the data was not graphed in the same method as the Ca and Ce XRF measurements. Instead, a two-sided t-test was performed on the two flow rates to determine if the increase in the carrier flow rate produced a difference in the observed Ga XRF counts. Based on the t-test, the average number of counts from a flow rate of 20 sccm of Ar was 27812 counts and the variance was 1.70×10^7 counts^2. From a flow rate of 23.6 sccm of Ar, the average number of counts was 34040 and the variance was 1.06×10^7 counts^2. The t-ratio was therefore -3.41, producing a p-value of 0.003. Thus, it is possible to see that increasing the flow rate of carrier gas through the Ga(tmhd)$_3$ bubbler made an expected increase in the number of observed Ga counts.

The EL performance of the materials is of particular interest. To simplify the analysis of the C.I.E. numbers which describe the chromatictity of the light emission in terms of a Cartesian x and y component pair, the C.I.E.'s were reduced to a single value of delta (δ). Delta can be visualized as the linear distance away from a desired color value. In the case of a blue color, the desired values are x=0.15 and y=0.20. So δ is calculated by:

$$\delta = \sqrt{(x - 0.15)^2 + (y - 0.20)^2}$$

This value could then be easily compared to specific properties of the deposition. The effect of the δ on the brightness of the coating is shown in Figure 3.

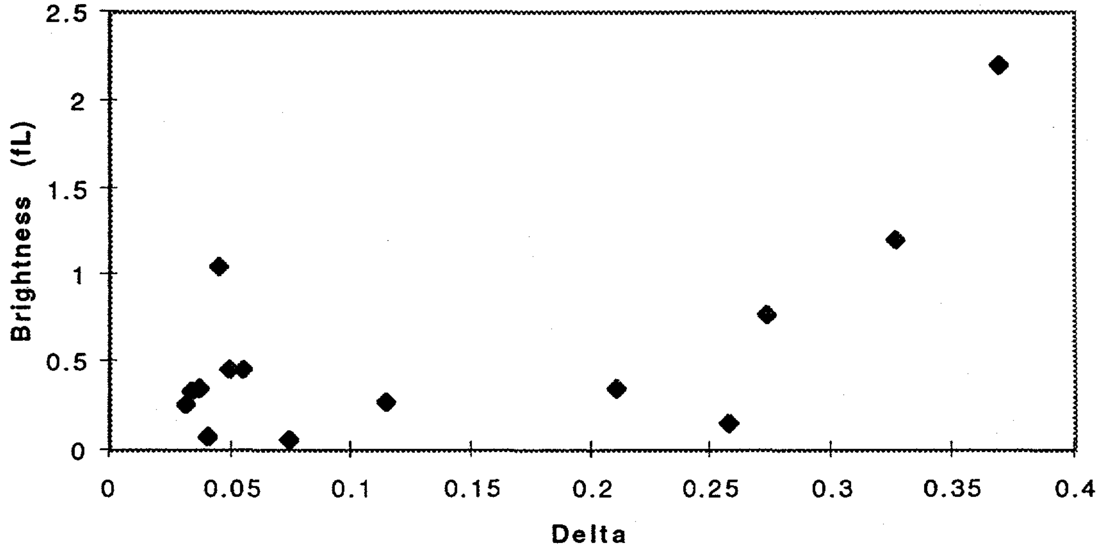

Figure 3. The increase in brightness as a function of delta (δ), the distance away from blue in color, is attributable to the presence of CaS:Ce in the deposition.

Within this graph, it is shown that at high values of δ the brightness increases sharply. This trend may be attributed to the presence of CaS:Ce in addition to $CaGa_2S_4$:Ce, either as a dispersed phase or as a layered composite. The output of pure CaS:Ce is significantly greater than that of $CaGa_2S_4$:Ce. Thus, small amounts of CaS:Ce can produce both the observed high brightness and a green shifted chromaticity. This change in the color of the luminescence is seen in the form of a high δ occurring since the green color is far away from the desired blue in terms of its C.I.E. values.

In characterizing the remaining samples, the best relationships were found in plotting the Ce/Ca Calibrated Ratio versus the Brightness, shown in Figure 4. The calibrated ratio of Ce to Ca was determined from the area of the XRF peaks multiplied by a calibration factor calculated from $CaGa_2S_4$ standards. To account for contributions to the XRF pattern by overlapping peaks from the indium and zinc which convoluted parts of the calcium and gallium peaks, respectively, a background pattern of the bare substrate was taken prior to deposition, and this pattern was subtracted from the measured pattern after deposition.

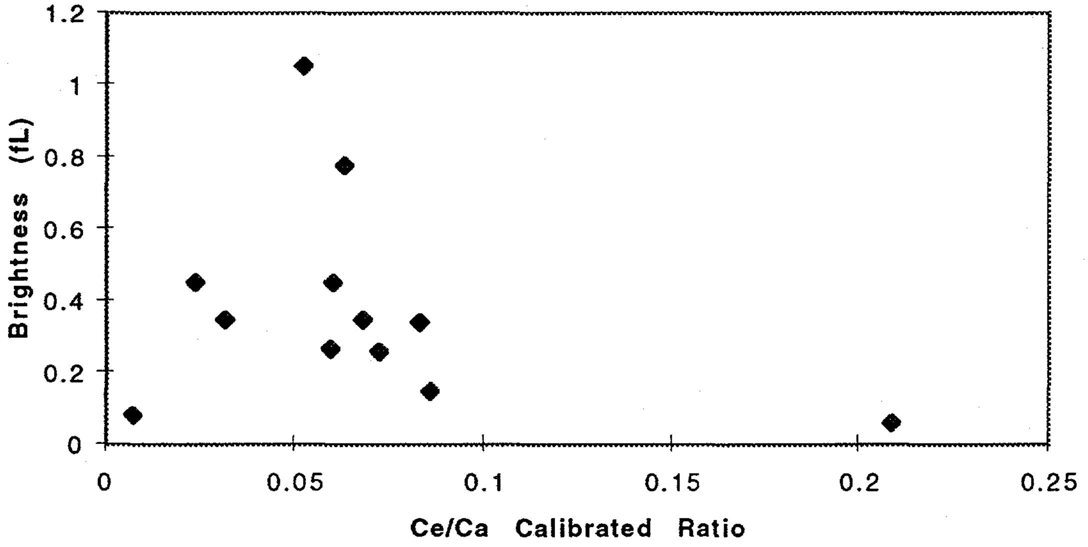

Figure 4. The optimum Ce doping level in $CaGa_2S_4$:Ce occurs at approximately 5 atomic percent.

Because these samples did not show significant evidence of excess CaS:Ce based on the δ and brightness values, it was assumed that all of the calcium present was in the form of $CaGa_2S_4$:Ce, and the excess gallium that was not in $CaGa_2S_4$:Ce was then assumed to be present as Ga_2S_3, a non-EL active phase. Therefore, the Ce/Ca Calibrated Ratio may then be assumed to be the degree of cerium doping within the luminescent phase.

Of particular interest in Figure 4 is the sharp peak which is present around a cerium doping of about 5 atomic percent. This experimental evidence would imply that the ideal doping for cerium would be approximately 5 atomic percent. Further, the quick rise and fall of the brightness at dopings just above and below 5 percent indicates that small deviations away from the ideal value can have significant effects on the brightness of the deposited material. It can therefore be determined that the cerium-doping which produces the highest brightness is about 5 atomic percent. This value corresponds well to values obtained from sputter deposition studies and would seem to indicate that the material produced by CVD does not differ significantly from that produced by PVD-type techniques.

Some of the other slight variation in Figure 4 in depositions with similar observed doping levels may be attributed to the presence of the excess Ga_2S_3 within the deposition. Since this phase is not active under electroluminescence conditions, it becomes essentially a dead area to the measurements. The brightness measurements are therefore lower than they would be if the deposited material were the pure-phase $CaGa_2S_4$:Ce, instead of the composite coating. Based on the analysis of the x-ray diffraction patterns from these samples, only slight variations in the observed Ga_2S_3 peaks were seen from sample to sample. Thus, the small variation in the brightness from samples with similar doping levels seen in Figure 4 can possibly be ascribed to the variation in the Ga_2S_3 content.

The effect of the cerium doping on the average unit cell volume can also be examined by using an estimate of the volume based on the XRD patterns. The possibility of the unit cell expansion is important in that it may be used to help explain the location of cerium within the unit cell. If it the Ce atom is at a substitutional atom position or at a grain boundary, no or only minimal unit cell deviation would be observed. If the Ce was interstitially positioned, an observable expansion of the unit cell would be expected. The estimates of the unit cell volume were determined by first indexing the XRD patterns for the $CaGa_2S_4$ phase. The peak positions and indices of those peaks, along with the crystal structure (in this case orthogonal) were entered into the program Unitcell[6] and used to estimate the unit cell parameters using a least squares refinement. The results from this program were in the form of the lattice parameters which could be used to calculate the volume of the unit cell. The graph of estimated unit cell volumes and Ce/Ca calibrated ratio is shown in Figure 5.

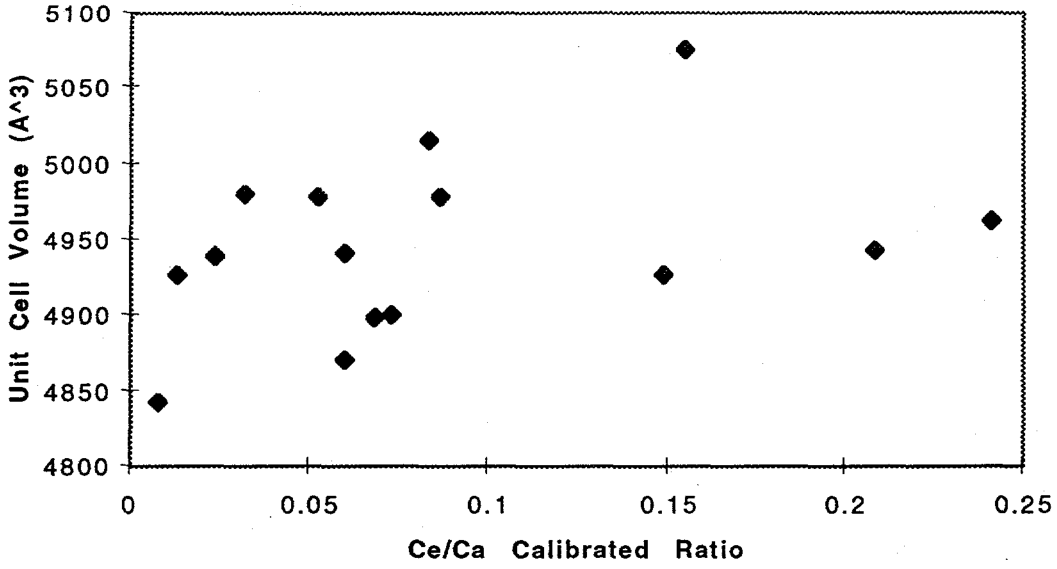

Figure 5. The estimated unit cell volume in Å^3 shows a weakly increasing relationship with the level of cerium doping.

It can be seen in this graph that there appears to be an overall trend in the unit cell volume as a function of the Ce/Ca calibrated ratio is a positive effect. That is to say that the calculated unit cell volume increases as the $CaGa_2S_4$ doping level is increased. However, the results of simple linear regression of these samples showed only a very weak relationship between these two quantities. The effect of the cerium doping was found to be 297 Å^3 with a standard deviation of 212 Å^3; the t-ratio for this effect was then 1.40 which results in a p value of 0.186. The constant from regression was calculated to be 4919 Å^3 with a standard deviation of 23 Å^3. The F-statistic for the significance of the regression was calculated to be 1.95, giving a p value on the significance of 0.186. In its entirety, the regression shows that there is a possible relationship with just over 80% significance between the doping level and the size of the average deposited unit cell. A possible explanation as to the poor statistical relationship might be that there is a slight influence of the cerium doping but the random variation in the calculated volumes is preventing clear estimation of the doping effect.

The possibility of this relationship should not be construed as the unit cell size increasing with the cerium doping level; rather, it should be viewed that as the number of cerium atoms in the deposition increases, a greater number of unit cells increase in size to accommodate the cerium. In turn, this increase in the number of unit cells which contain cerium atoms shifts the average unit cell size to a slightly higher value. The unit cell size should asymptotically approach an upper limit for the unit cell size as the cerium doping increases to the point where cerium atoms are present in all unit cells. The individual diffraction peaks from the $CaGa_2S_4$ were not checked for asymmetry, but it is anticipated that they should contain a detectable amount of low side asymmetry because of the distribution of unit cell volumes below their extended size. This check of the 00ℓ, h00, and hh0 type peaks is planned for future work, as is further investigation into the accuracy of the estimation of the unit cell volume by taking the sample displacement and transparency into account. This additional certainty of the peak locations should decrease the random variation in the calculated unit cell size and better determine the extent of the relationship between the cerium doping and the unit cell volume.

4. CONCLUSIONS

The results of this study demonstrate that it is possible to deposit $CaGa_2S_4$:Ce from an MOCVD technique using traditional reagent sublimation methods. This deposition was concluded to be $CaGa_2S_4$ based on indexing of XRD patterns. The consistency of the process was shown to be reasonable based on empirical analysis of the XRF measurements of the Ca, Ce, and Ga peaks. The EL performance of these samples illustrated the problems which can occur by the appearance of CaS:Ce in the films because of the very intense green color which is produced. The EL also showed that the ideal doping level is approximately 5 atomic percent, which produced a brightness of 1.05 fL. However, this brightness value would not appear to be the highest attainable brightness due to the incorporation of Ga_2S_3, which acts as a dead phase, along with the active $CaGa_2S_4$:Ce. The results of the regression did not reveal an effect of the cerium doping level on the unit cell volume, but the possibility of a relationship is still being investigated using more sensitive techniques to reduce the random variation of the measurements.

5. REFERENCES

1. W.A. Barrow, R.C. Coovert, E. Dickey, C.N. King, C. Laakso, S.S. Sun, R. Wentross, and J. King, SID 93 Digest, 761-764 (1993).

2. L.V. Pham, J.F. Wager, S.S. Sun, E. Dickey, R.T. Tunge, and C.N. King, SPIE--The International Society for Optical Engineering, Vol. 2174, P.S. Friedman, ed., 190-199 (1994).

3. S.S. Sun, R.T. Tunge, J. Kane, and M. Ling, J. Electrochem. Soc., 141, 2877-2883 (1994).

4. T.E. Peters and J.A. Baglio, J. Electrochem. Soc., 119, 230-236 (1972).

5. N.I. Yagubov, T.N. Guliev, P.G. Rustamov, and E.T. Azizov, Mat. Res. Bull. , 25, 271-276 (1990).

6. H. Toraya, J. Appl. Cryst., 26, 583-590 (1993).